Evaluation of Ranibizumab-Induced Changes in High-Resolution Optical Coherence Tomographic Retinal Morphology and Their Impact on Visual Function

Christopher G. Kiss,[1] *Wolfgang Geitzenauer,*[1] *Christian Simader,*[1] *Giovanni Gregori,*[2] *and Ursula Schmidt-Erfurth*[1]

Purpose. To evaluate the effects of intravitreal ranibizumab on retinal function and morphology and to identify a correlation between anatomy and function by using spectral domain optical coherence tomography (SDOCT).

Methods. Twenty-three patients affected by neovascular AMD received three injections of ranibizumab in three consecutive months and were monitored by assessment of best corrected visual acuity (BCVA), central retinal sensitivity (CRS) and morphologic changes at the level of the retina and the retinal pigment epithelium (RPE). The morphologic changes, identified by SDOCT segmentation, were mean retinal thickness (MRT), central retinal thickness (CRT), and the pathologic area (lesion area) of the RPE.

Results. BCVA increased from a mean 60.1 ± 8.7 letters at baseline to 67.0 ± 10.9 at month 3 ($P = 0.0003$). The CRS at the 0° position increased from 2.8 ± 3.1 dB at baseline to 4.0 ± 5.7 at week 1, remaining stable until month 3. Absolute scotoma size decreased continuously from baseline to month 3, in a mean of 5.3 ± 5.8 to 3.6 ± 4.0 test point locations. By SDOCT, MRT decreased from 308.6 ± 25.9 μm at baseline to 268.4 ± 22.4 μm at month 3 ($P = 0.0001$). CRT was 365.8 ± 84.9 and 254.9 ± 95.1 μm at month 3 ($P = 0.0002$). The mean RPE lesion area was 6.0 ± 3.0 mm^2 at baseline, which decreased to 5.0 ± 3.1 mm^2 at month 3 ($P = 0.115$). The only significant correlation was identified between the lesion area and CRS.

Conclusions. In ranibizumab therapy, the condition of the RPE lesion may be more relevant for visual function than the usual OCT parameters, retinal thickness. (*Invest Ophthalmol Vis Sci.* 2009;50:2376–2383) DOI:10.1167/iovs.08-2017

The development of choroidal neovascularization (CNV) secondary to age-related macular degeneration (AMD) is known to be triggered by the release of vascular endothelial growth factor (VEGF).[1–3] As Bruch's membrane and the choroidal microvasculature age, the metabolic and antioxidative mechanisms become insufficient. Inflammatory as well as oxidative conditions lead to an increased expression of VEGF and other angiogenic factors.[4] The resultant fibrovascular proliferation (i.e., CNV) induces the symptoms of exudative AMD and initiates a destructive sequence of events within the retina. The eradication of the pathogenic neovascular substrate therefore appears to be an adequate therapeutic approach to saving visual function.

The knowledge about the pathophysiologic role of VEGF and other proangiogenic mediators led to the development of inhibitors against these angiogenic factors. Efficacy and safety of intravitreal application of pegaptanib (Macugen; Pfizer, New York, NY),[5,6] and ranibizumab (Lucentis; Genentech, South San Francisco, CA)[7–9] have already been shown in clinical studies.

Ranibizumab, a humanized monoclonal antibody fragment, has been shown to be an effective inhibitor of all VEGF-A isoforms.[7,10] Several clinical studies have shown ranibizumab to be a safe and very effective treatment for choroidal neovascularization.[9,11–13] In these studies, the most pronounced effect on CNV leakage, retinal edema, and functional rehabilitation seems to occur within the initial therapeutic phase,[8,9] while the subsequent maintenance phase typically demonstrates a stable condition without substantial improvement or loss in visual function. However, the suggested monthly retreatment regimen represents a substantial burden for patients, treating doctors, and healthcare budgets. Therefore sensitive diagnostic parameters are needed to identify adequate biomarkers to guide (re)treatment indications. In the PrONTO study (Prospective OCT Study with Lucentis for Neovascular AMD), OCT was used to determine the effect of ranibizumab therapy on retinal structures and the need for retreatment. Investigators described an immediate therapeutic effect on retinal anatomy (i.e., a decrease in retinal thickness), as well as an associated increase in central retinal function, particularly at treatment initiation.[14]

Consequently, an evaluation of the early treatment response is of particular importance in understanding the impact of specific morphologic changes on neurosensory function and in identifying anatomic parameters offering a prognostic value for visual recovery. However, the role of central retinal thickness (CRT) by OCT is still discussed, and the data on correlation of CRT and visual acuity appear contradictory.[15] The main disadvantage of the current OCT technology is the fact that retinal thickness data are being computed from only six radial scans. The recently introduced spectral domain (SD)OCT technology offers the advantage of raster scanning the entire macular area at an axial resolution of ~5 μm. Parameters such as retinal thickness and retinal volume are thus computed from up to 256 neighboring slices without the need of surrogate interpolation. The acquisition of a detailed dataset of the posterior pole should facilitate the identification of morphologic parameters that realistically correlate with visual function during antiangiogenic therapy. The three-dimensional, high-resolution

From the [1]Department of Ophthalmology and Optometry at the Medical University of Vienna, Vienna, Austria; and the [2]Bascom Palmer Eye Institute, University of Miami Miller School of Medicine, Miami, Florida.

Supported by Carl Zeiss Meditec, which provided the SD-OCT unit, and Novartis Pharma, which provided the drug ranibizumab.

Submitted for publication March 12, 2008; revised June 25, August 23, and October 10, 2008; accepted March 16, 2009.

Disclosure: **C.G. Kiss**, Carl Zeiss Meditec (F), Novartis Pharma (F); **W. Geitzenauer**, Carl Zeiss Meditec (F), Novartis Pharma (F); **C. Simader**, Carl Zeiss Meditec (F), Novartis Pharma (F); **G. Gregori**, Carl Zeiss Meditec (F), Novartis Pharma (F); **U. Schmidt-Erfurth**, Carl Zeiss Meditec (F), Novartis Pharma (F)

The publication costs of this article were defrayed in part by page charge payment. This article must therefore be marked "*advertisement*" in accordance with 18 U.S.C. §1734 solely to indicate this fact.

Corresponding author: Christopher G. Kiss, Department of Ophthalmology and Optometry, Medical University of Vienna, Waehringer Grtl. 18-20, A-1090 Vienna, Austria; christopher.kiss@meduniwien.ac.at.

modality facilitates the identification of additional morphologic features by using segmentation algorithms to detect not only retinal but also RPE disease. Hence, the underlying condition of retinal leakage (i.e., the neovascular RPE lesion) can be identified and quantified in its morphology and extension. Taking advantage of this novel method of image acquisition and retinal layer segmentation, the present study was designed to identify the specific anatomic effects of intravitreal ranibizumab therapy in patients with CNV secondary to AMD. Furthermore, an exact evaluation of visual function (i.e., visual acuity and central retinal sensitivity), was performed and correlated to the OCT–morphologic parameters.

METHODS

From January to August 2006, 53 patients of the retina service at the Department of Ophthalmology and Optometry, Medical University of Vienna, were screened. Of these 29 patients fulfilled the inclusion criteria and were included in the study, but only 23 eyes of 23 patients were included into the present analysis. Six patients were excluded, either because follow-up (3 months) was incomplete or OCT scan quality was not sufficient at all visits, precluding reliable analyses. The protocol adhered to the tenets of the Declaration of Helsinki and was approved by the local ethics committee. Written informed consent was obtained from all individuals after a detailed discussion of the nature and possible consequences of the study procedures.

Patient Eligibility

Patients aged 50 years or older, showing angiographic evidence of CNV secondary to AMD were included in the study. Baseline fluorescein angiography was performed using the HRA2 (Heidelberg Engineering, Dossenheim, Germany) after intravenous injection of a 5% fluorescein solution. All exudative lesion types—predominantly classic, minimally classic, and occult with no classic components—were permitted. The best corrected visual acuity (BCVA) score, assessed by using the Early Treatment Diabetic Retinopathy Study (ETDRS) protocol, ranged between 24 and 74 letters. Previous photodynamic therapy, transpupillary thermotherapy, and antiangiogenic or retinal laser treatment were exclusion criteria. Patients with media opacities, a pigment epithelial detachment or hemorrhage larger than 50% of the lesion as well as patients with subfoveal fibrosis, a history of submacular surgery or uncontrolled glaucoma or CNV due to causes other than AMD were also excluded.

Ranibizumab Treatment

All included patients received standard intravitreal injections with ranibizumab at baseline and routinely at months 1 and 2. Under sterile conditions, a volume of 0.05 mL (0.3 mg) ranibizumab was injected intravitreally after topical anesthesia using 2% oxybuprocaine and conjunctival instillation of 5% povidone iodine drops. Patients were instructed to self-administer gentamicin eye drops daily for 1 week after injection.

Assessment of Retinal Function

Functional retinal changes were assessed by testing BCVA at baseline, week 1 and months 1, 2, and 3. Refraction and BCVA scores on ETDRS charts were documented.

At the same visits, microperimetry was performed (Microperimeter MP-1; Nidek Technologies, Padova, Italy), a fundus-controlled device including an eye-tracking system that allows for fully automated assessment of central macular sensitivity.[16–19] Furthermore, a delineation of absolute scotoma was performed. The stimulation pattern consisted of 25 stimulation loci: a central point (0°) and two circles of 12 points each at 3.5° and 7.9° to specifically test for a central (0°), paracentral (3.5°), and eccentric (7.9°) sensitivity. The stimulus-size was Goldmann III, presented for a time-interval of 200 ms. The background color was white and the background luminance was 1.27 cd/m^2. Differential threshold values were obtained with a 4-2-1 staircase strategy. A red 7° circle was used as fixation the mark. If the patient was unable to identify the 7° circle, the size was increased in 1° steps until stable fixation was achieved.

Documentation of Retinal and RPE Morphology

Distinct morphologic retinal changes were identified by high-resolution, spectral-domain optical coherence tomography (SDOCT) at baseline, week 1, and months 1, 2, and 3 using a standardized protocol: Each eye was scanned at least twice during the examination and instantly reviewed regarding signal strength, scan centration, and eye movements. Only the best scan out of this set was included in the analysis.

All examinations were performed using a Cirrus-prototype (Carl Zeiss Meditec Inc., Dublin, CA). In contrast to the standard time-domain technology used by conventional Stratus OCT, the spectral domain technology of the prototype allowed the acquisition of a complete three-dimensional dataset of the posterior pole (6×6 mm) with an axial resolution of 5 μm. The scanning module used a broad-spectrum superluminescent diode (SLD) with an 840-nm center wavelength and was capable of acquiring 27,000 A-scans/s. Simultaneous fundus observation was achieved via a line-scanning laser ophthalmoscope (LSLO) consisting of an SLD with a 750-nm wavelength. For statistical analysis of posterior pole characteristics, a stack of 256 images consisting of 256 A-scans was recorded in approximately 2.4 seconds (as opposed to the prototype, the commercial Cirrus offers a 200×200 scan). For detailed evaluation of retinal layering in the foveola, three lines consisting of 4096 A-scans were acquired. A novel algorithm was used to analyze the 256×256 stack of data and to quantify the mean retinal thickness (MRT), retinal thickness of the central circle of 1-mm diameter (CRT) and the area of disease in the RPE, referred to as the lesion area. The area was defined as the site presenting a significant deviation in RPE contour at the location of the subretinal disease (e.g., a neovascular membrane or fibrovascular RPE detachment from the physiologic continuity of the adjacent intact RPE layer; Fig. 1). This algorithm has been investigated regarding accuracy compared with hand-drawn segmentation (Weisbrod M, et al. *IOVS* 2008;49:ARVO E-Abstract 4240), reproducibility (Gregori G, et al. *IOVS* 2007;48:ARVO E-Abstract 153), and clinical applicability.[20] As shown in Figure 1, the algorithm determined the internal limiting membrane (ILM) as the inner and the RPE as the outer border for its calculation of morphologic parameters. Sub- and intraretinal fluid, for example, would be included in the MRT and CRT measurements, whereas sub-RPE fluid would not be included. Every scan was evaluated regarding scan centration compared with that in the previous visit (where applicable) and quality of the segmentation. Errors of the segmentation algorithm were accepted if less than 5% of the B-scans were affected. Scans showing elevations of the RPE outside of the actual lesions were not accepted to avoid distortion in the calculation of the actual lesion size.

Statistical Analysis

The Mann-Whitney *U* and ANOVA tests were used for statistical analysis of changes in BCVA, in retinal threshold sensitivity, and in MRT, CRT, and lesion area compared with baseline. Associations between parameters were tested by calculating Pearson's correlation coefficient. $P \leq 0.05$ or less was considered statistically significant. If not indicated otherwise, all values are given as the mean $\pm$ SD.

RESULTS

Twenty-three eyes of 23 patients referred with active CNV due to AMD were included to the analysis; 13 (56.5%) were men, 10 (43.5%) were women. The mean age was 77.6 $\pm$ 7.6 years. Nine had predominantly classic lesions, seven had minimally

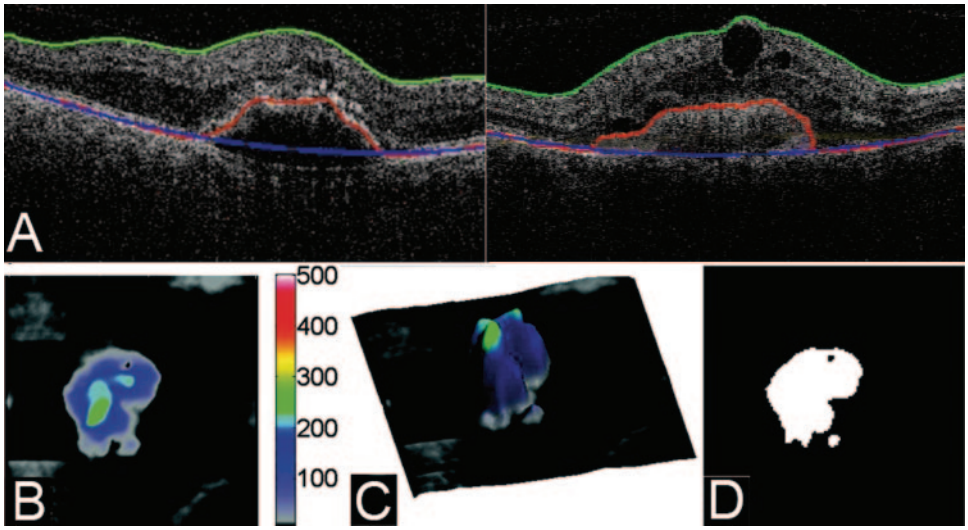

FIGURE 1. Automated analysis of the morphologic condition of the retina and RPE. Each B-scan of the scanned volume is separately segmented: (**A**) Examples of the segmentation for sub-RPE (*left*) and pre-RPE (*right*) lesions. *Green line*: internal limiting membrane (ILM); *blue line*: delineates and extrapolates the contour of intact physiologic RPE; *red line*: pathologic deviation of the RPE. A color-coded map of the RPE (**B**) is calculated from differences between the *red* (pathologic) and *blue* (physiologic) lines of each segmented B-scan at each RPE location. The map is represented as a three-dimensional relief (**C**). The location and extension of pathologic RPE deviation, referred to as the RPE lesion, is represented separately (**D**).

classic ones, and seven had occult lesions. Table 1 shows an overview of selected parameters for each patient.

Effect of Ranibizumab Treatment on Visual Parameters

BCVA data showed an immediate and significant improvement from a mean of 60.1 ± 8.7 letters at baseline to 65.5 ± 8.7 letters ($P = 0.000,002$) after 1 week and increased to 67.0 ± 10.9 letters at month 3 ($P = 0.0003$, Fig. 2).

The overall mean retinal sensitivity of the entire tested field was 5.8 ± 3.4 dB at baseline. An increase to 6.6 ± 3.4 ($P = 0.097$) after 1 week was documented that slightly decreased at month 3 to 6.2 ± 2.9 dB ($P = 0.382$). However, a separate analysis of the center test location (0°) and the test locations at 3.5° and 7.9° apart from the foveal center revealed a different pattern: At the center position (0°) the mean retinal sensitivity increased from 2.8 ± 3.1 dB at baseline to 4.0 ± 5.7 at week 1, remaining stable until month 3 with 4.0 ± 5.2 dB; 3.5° apart from the fovea, a similar pattern was observed. The retinal sensitivity increased from 4.6 ± 3.5 dB at baseline to 5.6 ± 4.1 dB at week 1, again remaining stable until month 3 at 5.6 ± 3.2 dB. At the 7.9° location a discrete decrease in mean retinal sensitivity was observed. The differential light threshold was 7.2 ± 3.7 dB at baseline and showed a slight increase to 7.8 ± 3.3 dB at week 1; but after 3 months, extrafoveal retinal sensitivity was lower than baseline at 6.9 ± 3.0 dB (Fig. 3).

The size of the absolute scotoma decreased continuously from baseline until month 3 from a mean of 5.3 ± 5.8 to 3.6 ± 4.0 test point locations (Fig. 4). At baseline 91.3% ($n = 21$) of all patients demonstrated an absolute scotoma at a level of ≥1 test point. At month 3, this proportion of eyes had decreased to 79.3% ($n = 18$).

TABLE 1. Functional and Anatomic Results of All Patients over Time

Baseline				Week 1				Month 1				Month 2				Month 3			
VA	dB	CRT	Area	VA	dB	CRT	Area	VA	dB	CRT	Area	VA	dB	CRT	Area	VA	dB	CRT	Area
61	4.0	403	6.6	73	3.0	340	7.0	72	4.2	342	8.5	60	5.4	319	6.3	57	4.4	292	6.8
67	3.6	336	11.2	64	4.1	283	11.5	66	3.0	204	10.7	49	5.1	222	9.2	69	5.2	202	6.2
47	3.3	357	6.9	56	10.1	298	6.4	55	6.5	79	6.2	52	4.4	310	7.5	56	5.4	270	7.3
71	7.9	295	6.5	80	10.2	217	7.8	83	11.0	274	7.2	83	12.7	241	7.0	83	9.6	259	6.3
65	12.1	284	3.2	71	10.0	237	3.0	66	7.6	220	2.9	65	8.7	182	2.4	65	6.6	229	3.0
56	9.2	496	9.1	61	7.0	269	6.2	57	8.6	256	5.3	53	8.5	230	3.8	51	7.8	218	3.9
47	1.6	495	8.8	47	2.1	261	8.1	48	3.8	355	7.2	46	2.6	244	8.6	40	2.6	237	8.6
56	0.0	460	4.0	60	2.9	375	2.6	57	5.5	295	3.5	55	3.0	250	3.6	65	1.3	253	3.9
51	9.7	388	3.3	63	8.8	265	2.5	66	12.2	272	2.9	62	11.8	177	2.9	61	9.3	178	1.8
68	10.6	362	2.3	74	13.8	338	1.8	73	10.8	309	1.9	71	13.7	293	2.4	73	12.0	296	2.5
63	2.4	321	3.2	68	4.1	301	4.8	69	6.4	279	5.4	78	6.2	226	5.6	77	4.0	169	4.4
68	9.8	386	2.3	69	8.7	298	2.3	71	8.4	362	2.7	72	4.5	322	3.0	73	5.8	287	2.5
71	6.4	355	5.2	78	7.8	375	6.5	70	9.2	329	5.4	71	8.6	309	5.3	72	7.2	242	5.5
58	5.8	378	6.1	67	8.5	170	3.6	63	6.2	243	3.4	68	5.2	221	2.2	68	10.2	223	2.7
69	4.1	517	9.9	72	6.0	517	7.0	72	5.2	688	4.5	68	4.5	485	3.4	72	2.8	595	8.8
55	2.6	302	6.9	61	4.6	251	4.7	60	5.7	311	5.5	56	5.3	287	5.5	68	5.2	286	5.2
54	6.5	290	10.1	56	5.7	253	7.3	58	2.2	188	1.1	64	8.0	139	3.7	63	7.9	156	2.6
66	6.3	335	9.1	68	2.7	295	7.3	67	6.4	397	6.8	66	6.4	272	6.1	74	4.1	252	6.4
56	0.8	368	9.7	63	0.6	278	10.2	63	0.9	260	10.7	62	0.6	270	11.2	63	2.2	213	12.4
69	8.5	411	3.3	75	11.0	300	0.9	76	10.6	180	1.5	83	10.7	221	1.2	80	8.7	231	1.5
73	9.2	430	1.1	73	9.8	422	0.6	73	10.9	285	1.0	80	11.4	250	1.0	85	8.9	245	1.1
57	2.8	144	4.6	58	5.8	217	3.0	53	5.3	302	3.9	57	1.8	293	2.9	60	3.6	238	2.7
42	5.2	315	5.6	49	4.2	286	5.7	54	7.0	252	6.0	53	3.3	309	6.1	55	6.8	291	7.9

VA, best-corrected visual acuity; dB, mean macular sensitivity; CRT, mean retinal thickness of the central 1-mm; Area, size of the RPE pathology.

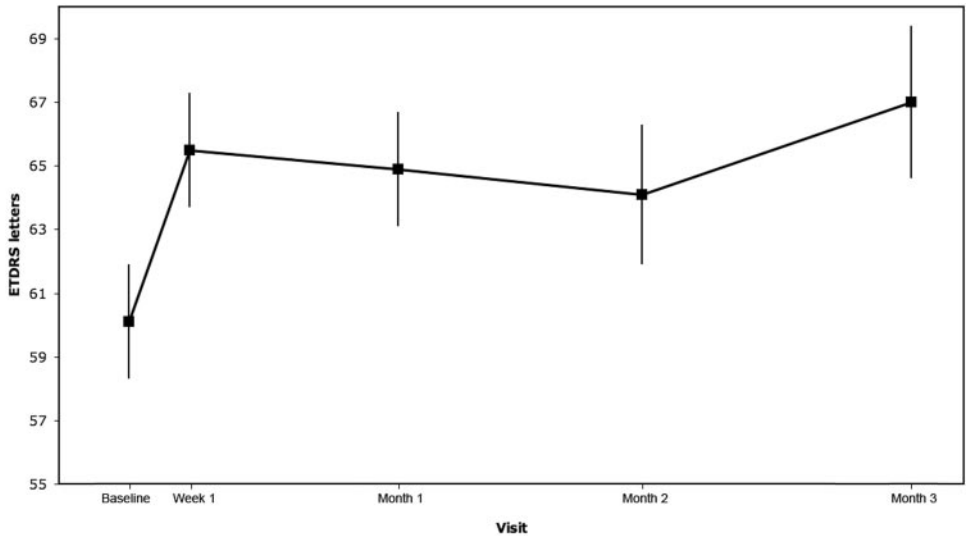

FIGURE 2. BCVA. Visual acuity data (ETDRS letters) revealed a rapid and continued increase during the 3-month observation period after administration of injections in three consecutive months.

SDOCT Analysis of Retinal and RPE Morphology

MRT of the central 6 × 6-mm area of the retina decreased from 308.6 ± 25.9 μm (median: 309.8) at baseline to 285.7 ± 25.9 μm after 1 week and further to 268.4 ± 22.4 μm at month 3 ($P = 0.0001$, Fig. 5, boxes).

CRT at the fovea (i.e., the central 1 mm, was 365.8 ± 84.9 μm at baseline), decreased to 298.2 ± 84.0 μm after 1 week, and was at 254.9 ± 95.1 μm at month 3 ($P = 0.0002$; Fig. 5, circles).

A mean lesion area (i.e., area of pathologic RPE) deviation of 6.0 ± 3.0 mm^2 was identified at baseline, whereas a decrease to 5.2 ± 3.1 and 5.0 ± 3.1 mm^2 was documented at week 1 and month 3, respectively ($P = 0.115$, Fig. 6).

Correlation of Morphologic and Visual Parameters

A representative composite of associated effects on retinal thickness, area of RPE lesion, and retinal sensitivity is presented in Figure 7. Over time, retinal edema resolved progressively, the RPE lesion became flatter, and the area of RPE lesion demonstrated an obvious change in anatomic configuration and size. Accordingly, BCVA and retinal sensitivity, as functional parameters, improved. Analysis of the relationship between VA results and the parameters acquired by SDOCT revealed no significant influence of any of the common OCT parameters such as MRT and CRT on visual function. The only significant correlation between morphology and function was found between RPE lesion area and central retinal sensitivity (Table 2).

DISCUSSION

The purpose of this study was to investigate the direct effects on retinal and RPE morphology as well as visual function after intravitreal ranibizumab therapy for CNV in AMD. The immediate effect of intravitreal ranibizumab on retinal anatomy, as seen by the standard OCT technology, has been proven by Fung et al.,[14] who reported an immediate resolution of sub- and intraretinal fluid. Since the information on retinal and subretinal morphology is limited by the low resolution and particularly the hardly reproducible location of a few radial scans of conventional OCT, the purpose of the present study was to use the novel spectral-domain technology offering an all-location raster scanning mode, improved resolution, and segmentation algorithms for retinal as well as RPE layers. Accordingly, in our study population, a rapid decrease in all

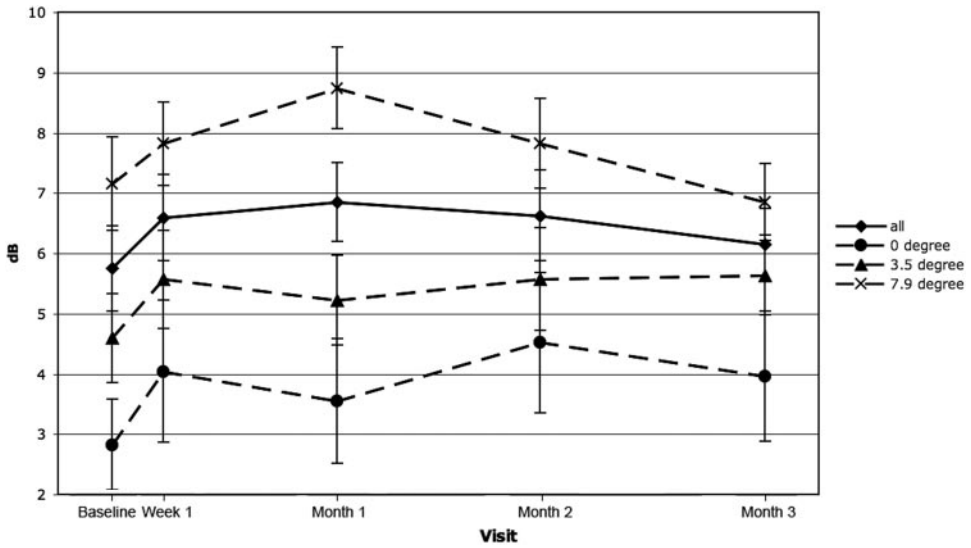

FIGURE 3. Retinal sensitivity. Retinal sensitivity (*circles*) demonstrated an overall improvement after therapy. The functional benefit is most pronounced at the central foveal location (0°) and pericentrally (3.5°). At a more peripheral location of 7.9°, retinal function does not reveal an increase in sensitivity.

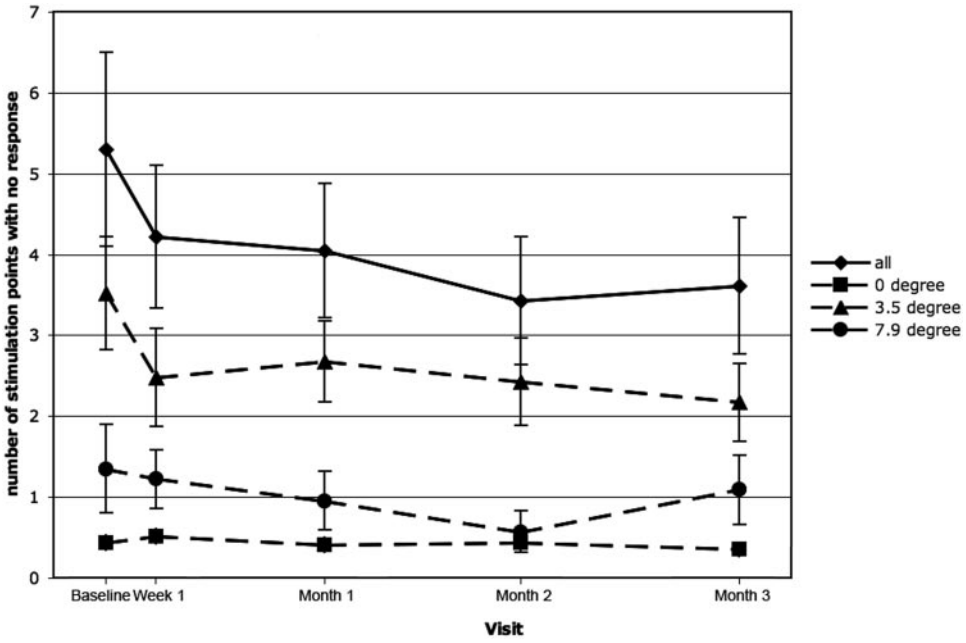

FIGURE 4. Absolute scotoma. The size of absolute scotoma decreased continuously over time and remained remarkably smaller at 3 months than at baseline. The extension of the absolute scotoma was quantified as the number of test locations not recognized by the patient at the highest stimulus intensity.

parameters of pathologic retinal morphology (i.e., central and mean retinal thickness), was observed. However, a more comprehensive insight into treatment-related therapeutic effects becomes available using currently available SDOCT methods. Most important, the precise geography of retinal thickening becomes obvious since all obtained raster scans provided real on-site measurements without the imprecision of extrapolation of missing data.[21] However, although certain limitations inherent to all studies involving OCT measurements remain (i.e., computed parameters are dependent on scan centration and motion artifacts), they are minimized through the shorter acquisition times of the SDOCT system, enabling a more precise calculation. A second and completely novel aspect is clearly the identification of the morphology of the primary lesion site. A delineation of the lesion configuration and exact extension of the subretinal disease is not accessible with any standard OCT system. Clearly, the underlying RPE disease harboring the CNV lesion reflects the pathophysiology of neovascular AMD much more than it reflects the secondary consequences, such as intraretinal edema and subretinal fluid. Identification of the characteristics of the subretinal lesion offers novel insight into the biology of neovascular AMD and the mechanisms of anti-VEGF therapy. In our study, it appears that ranibizumab rapidly diminishes the leakage activity of the neovascular net and at a slower pace has a direct impact on the morphology of the RPE lesion as the subretinal lesion flattens progressively and the abnormal RPE area decreased in size during the initial treatment phase when visual function is affected positively in 80% of treated eyes.[9] However, in none of the tested eyes did the RPE lesion disappear completely. Obviously, resolution of fluid within the diseased area of the RPE may play a role in the morphologic change of an RPE prominence, and it remains to be proven that the area and surface contour of the identified pathologic area in the RPE is truly consistent with the CNV lesion itself. In a separate study, we performed an analysis of 61 baseline CNV cases and scans including corresponding angio-

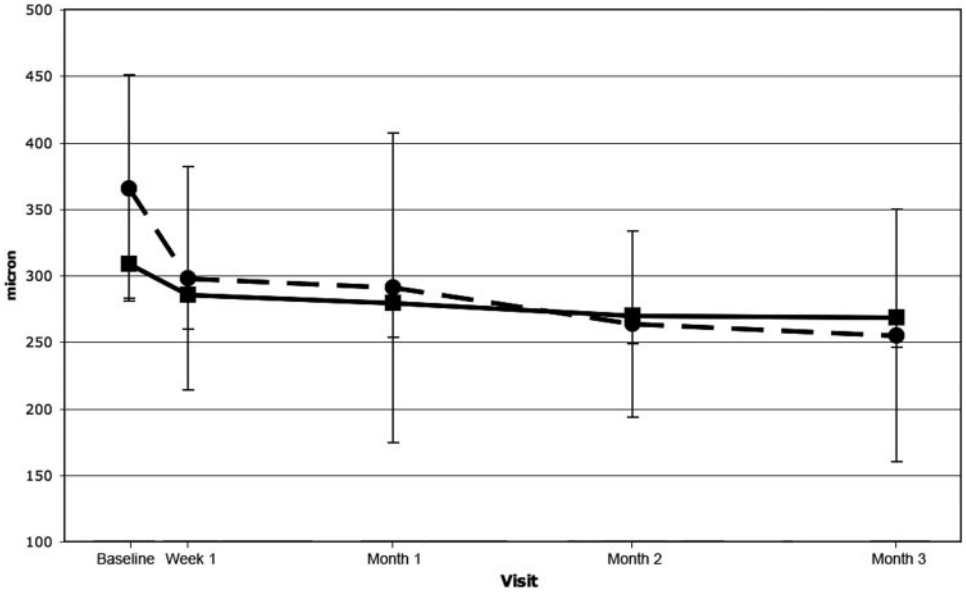

FIGURE 5. Morphologic parameters as assessed by high-resolution OCT. MRT of the total scanned volume (■) and thickness of the 1-mm CRT (●) showed a continuous decrease over time.

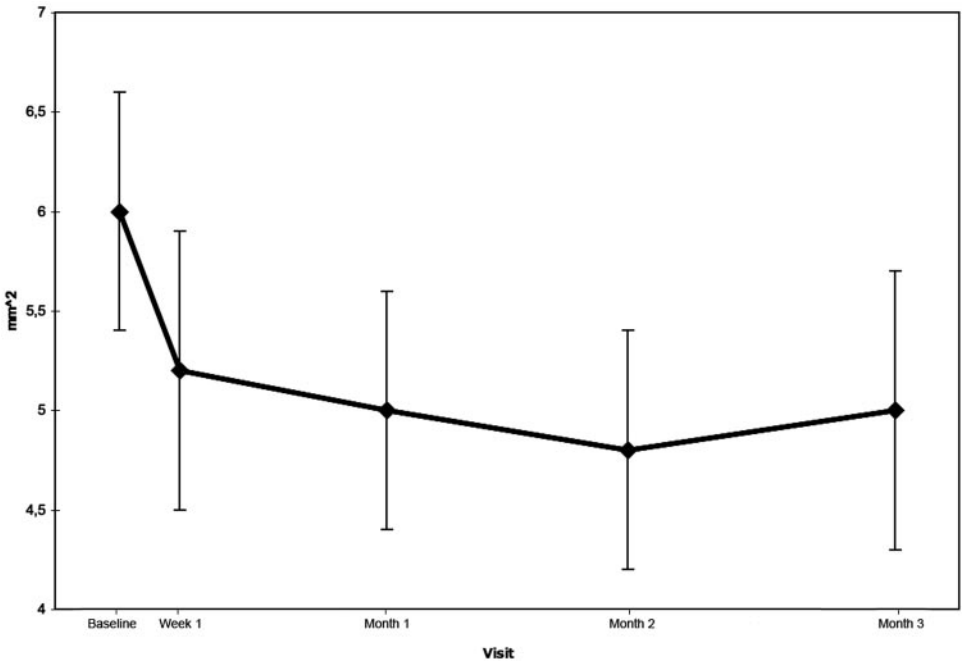

FIGURE 6. Morphologic parameters as assessed by high-resolution OCT. The size of the abnormal area of the RPE became smaller, especially during the first 2 months and remained stable thereafter.

graphic features: A good correlation between all pathologic conditions in the RPE identified by SDOCT with the angiographic location of the neovascular process was noted (Kiss CG, et al., manuscript in preparation). In addition, in our cases the scan segmentation following the contour of the pathologic RPE was identical with the surface reflectivity of the neovas-

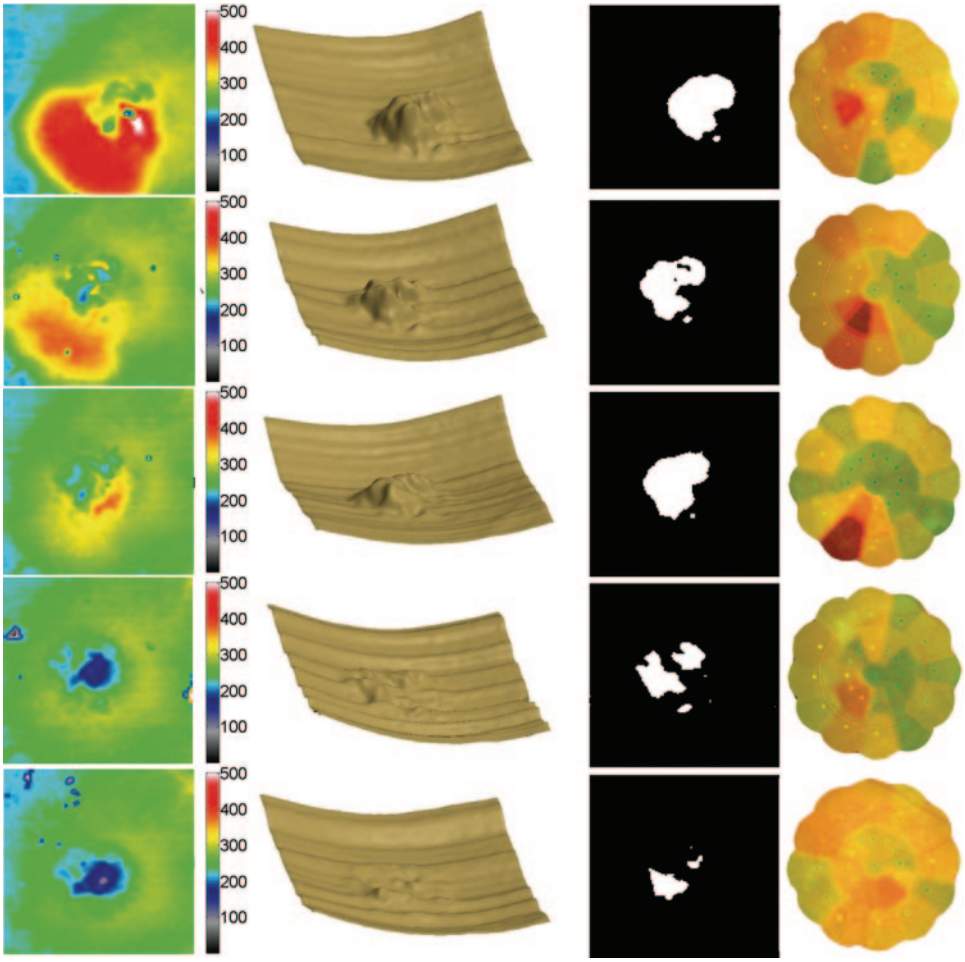

FIGURE 7. Illustration of retinal and RPE-related morphologic changes and retinal function. The first column shows a favorable development of the retinal thickness map appearance after ranibizumab therapy. The second and third columns represent the change in the morphology of the configuration (*left*) and extent (*right*) of the pathologic area. The retinal and the RPE diseased areas seem to correlate with the functional map obtained by the automated macular perimetry shown in the fourth column and with the BCVA scores with respect to the location of the functional deficit.

TABLE 2. Correlation Coefficient for the Evaluation of the Relationship between the RPE Lesion Area and CRS

	Baseline	Week 1	Month 1	Month 2	Month 3
Lesion area (mm^2)	6.0 ± 3.0	5.2 ± 3.1	4.9 ± 2.9	4.8 ± 2.8	5.0 ± 3.1
CRS (dB)	5.8 ± 3.4	6.6 ± 3.4	6.9 ± 3.0	6.6 ± 3.6	6.2 ± 2.9
r	−0.447	−0.619	−0.508	−0.491	−0.631
P	0.037	0.005	0.026	0.020	0.004

cular complex in cases of classic CNV and the fibrovascular RPE elevation in cases of occult CNV components. However, these were selected cases depending on good compliance by the patient. Only patients showing fairly stable fixation and no head movement were included in the present analysis to ensure proper scan centration and to avoid artifacts and subsequent algorithm errors. Furthermore, multiple scans were taken at each visit and only the best one was selected, because all the aforementioned issues could otherwise seriously influence the data. In the clinical routine, a manual correction of the segmentation might be necessary. Overall, the change in lesion morphology was consistently monitored by SDOCT and revealed a progressive decrease in prominence and area.

The most intriguing aspect of our findings is the role of RPE lesion morphology in visual function. The only morphologic feature, which was found to correlate with retinal sensitivity as a parameter of visual performance, was the size of the abnormal area. No correlation was noted between morphologic parameters and ETDRS visual acuity. It could therefore be hypothesized that the condition of the RPE as measured by high-resolution OCT may be an indirect indicator of overlying photoreceptor dysfunction[22] and is thus more important for visual function than frequently used parameters such as central retinal thickness or retinal volume.

Visual function includes multiple aspects with respect to the type of psychophysical measurement such as BCVA testing, scotometry, and multifocal ERG. Although previous studies concentrated on either visual acuity or contrast sensitivity, our study also monitored retinal sensitivity as assessed by fundus-controlled microperimetry. A discrepancy between the recovery of visual acuity and retinal sensitivity after ranibizumab therapy was noted: although VA showed a remarkable improvement, the overall retinal sensitivity did not recover consistently. The discrepancy between VA and CRS was attributable to the possible learning process of visually impaired patients, in which a shift of the preferred retinal locus (PRL) has been described.[23] Thus, VA scores can be quite good, whereas higher order visual functions such as reading remain impaired.[24] The high-resolution SDOCT offers an important advantage over standard OCT which offers a detailed evaluation of the RPE lesion at each location. It is not surprising that the condition of the RPE is critical to the visual outcome. Our group has recently been able to show that the commonly used retinal thickness measurement may not be reliable in certain retinal diseases as a predictive parameter for visual function.[25]

Midena et al.[16] also recently showed that macular sensitivity significantly decreases over large drusen (11.2 ± 5.6 dB, $P < 0.0001$) and over RPE abnormalities (13.1 ± 3.6 dB, $P < 0.0001$). When both characteristics were present, the reduction was highest when compared to the absence of those factors (9.6 ± 4.3 dB vs. 15.0 ± 4.5 dB; $P < 0.0001$). This finding further stresses the superiority of RPE analysis over mere estimation of retinal thickness or volume, as also reflected by our data obtained in a study of patients with CNV.

Tezel et al.[26] extensively investigated the relationship between retinal sensitivity and underlying retinal anatomy and found that the relative risk of an absolute scotoma is highest over areas of chorioretinal scars, RPE atrophy, subretinal hemorrhage, and the neovascular membrane with its destructive growth. The importance of the RPE condition is further highlighted by Schneider et al.,[27] who found that eyes with classic CNV had deeper scotomas than eyes with occult CNV.

The immediate effects of ranibizumab therapy documented by SDOCT are in concordance to previous reports using StratusOCT. However, the analysis of computed parameters of retinal anatomy and the relation to visual function indicate that the commonly used parameter of retinal thickness may not be sufficient for correlating retinal morphology and visual function when the extent of the subretinal lesion is not determined. The improved resolution provided by high-resolution SDOCT for morphologic evaluation, together with adequate parameters of retinal function, may help to facilitate diagnosis and development of treatment regimens for patients with neovascular AMD in the era of antiangiogenic therapy.

References

1. Kvanta A, Algvere PV, Berglin L, Seregard S. Subfoveal fibrovascular membranes in age-related macular degeneration express vascular endothelial growth factor. *Invest Ophthalmol Vis Sci.* 1996;37:1929–1934.
2. Lopez PF, Sippy BD, Lambert HM, Thach AB, Hinton DR. Transdifferentiated retinal pigment epithelial cells are immunoreactive for vascular endothelial growth factor in surgically excised age- related macular degeneration-related choroidal neovascular membranes. *Invest Ophthalmol Vis Sci.* 1996;37:855–868.
3. Cui JZ, Kimura H, Spee C, Thumann G, Hinton DR, Ryan SJ. Natural history of choroidal neovascularization induced by vascular endothelial growth factor in the primate. *Graefes Arch Clin Exp Ophthalmol.* 2000;238:326–333.
4. Beatty S, Koh H, Phil M, Henson D, Boulton M. The role of oxidative stress in the pathogenesis of age-related macular degeneration. *Surv Ophthalmol.* 2000;45:115–134.
5. Chakravarthy U, Adamis AP, Cunningham ET Jr, et al. Year 2 efficacy results of 2 randomized controlled clinical trials of pegaptanib for neovascular age-related macular degeneration. *Ophthalmology.* 2006;113:1508 e1501–1525.
6. D'Amico DJ, Patel M, Adamis AP, Cunningham ET Jr, Guyer DR, Katz B. Pegaptanib sodium for neovascular age-related macular degeneration: two-year safety results of the two prospective, multicenter, controlled clinical trials. *Ophthalmology.* 2006;113:1001,e1001–e1006.
7. Ferrara N, Damico L, Shams N, Lowman H, Kim R. Development of ranibizumab, an anti-vascular endothelial growth factor antigen binding fragment, as therapy for neovascular age-related macular degeneration. *Retina.* 2006;26:859–870.
8. Heier JS, Antoszyk AN, Pavan PR, et al. Ranibizumab for treatment of neovascular age-related macular degeneration: a phase I/II multicenter, controlled, multidose study. *Ophthalmology.* 2006;113:642 e641–644.
9. Rosenfeld PJ, Brown DM, Heier JS, et al. Ranibizumab for neovascular age-related macular degeneration. *N Engl J Med.* 2006;355:1419–1431.
10. Krzystolik MG, Afshari MA, Adamis AP, et al. Prevention of experimental choroidal neovascularization with intravitreal anti-vascular endothelial growth factor antibody fragment. *Arch Ophthalmol.* 2002;120:338–346.
11. Rosenfeld PJ, Heier JS, Hantsbarger G, Shams N. Tolerability and efficacy of multiple escalating doses of ranibizumab (Lucentis) for

neovascular age-related macular degeneration. *Ophthalmology.* 2006;113:632 e631.

12. Rosenfeld PJ, Schwartz SD, Blumenkranz MS, et al. Maximum tolerated dose of a humanized anti-vascular endothelial growth factor antibody fragment for treating neovascular age-related macular degeneration. *Ophthalmology.* 2005;112:1048–1053.
13. Heier JS, Rosenfeld PJ, Antoszyk AN, Hantsbarger G, Kim R, Shams N. Long-term experience with Lucentis (ranibizumab) in patients with neovascular age-related macular degeneration (AMD). *Invest Ophthalmol Vis Sci.* 2005;46:1393-.
14. Fung AE, Lalwani GA, Rosenfeld PJ, et al. An optical coherence tomography-guided, variable dosing regimen with intravitreal ranibizumab (Lucentis) for neovascular age-related macular degeneration. *Am J Ophthalmol.* 2007;143:566–583.
15. Moutray T, Alarbi M, Mahon G, Stevenson M, Chakravarthy U. Relationships between clinical measures of visual function, fluorescein angiographic and optical coherence tomography features in patients with subfoveal choroidal neovascularisation. *Br J Ophthalmol.* 2008;92:361–364.
16. Midena E, Vujosevic S, Convento E, Manfre A, Cavarzeran F, Pilotto E. Microperimetry and fundus autofluorescence in patients with early age-related macular degeneration. *Br J Ophthalmol.* 2007;91:1499–1503.
17. Springer C, Bultmann S, Volcker HE, Rohrschneider K. Fundus perimetry with the micro perimeter 1 in normal individuals: comparison with conventional threshold perimetry. *Ophthalmology.* 2005;112:848–854.
18. Midena E, Radin PP, Pilotto E, Ghirlando A, Convento E, Varano M. Fixation pattern and macular sensitivity in eyes with subfoveal choroidal neovascularization secondary to age-related macular degeneration: a microperimetry study. *Semin Ophthalmol.* 2004;19:55–61.
19. Rohrschneider K, Springer C, Bultmann S, Volcker HE. Microperimetry: comparison between the micro perimeter 1 and scanning laser ophthalmoscope–fundus perimetry. *Am J Ophthalmol.* 2005;139:125–134.
20. Legaretta JE, Gregori G, Knighton RW, Punjabi OS, Lalwani GA, Puliafito CA. Three-dimensional spectral-domain optical coherence tomography images of the retina in the presence of epiretinal membranes. *Am J Ophthalmol.* 2008;145:1023–1030.
21. Leung CK, Cheung CY, Weinreb RN, et al. Comparison of macular thickness measurements between time domain and spectral domain optical coherence tomography. *Invest Ophthalmol Vis Sci.* 2008;49(11):4893–4897.
22. Strauss O. The retinal pigment epithelium in visual function. *Physiol Rev.* 2005;85:845–881.
23. Timberlake GT, Peli E, Essock EA, Augliere RA. Reading with a macular scotoma. II. Retinal locus for scanning text. *Invest Ophthalmol Vis Sci.* 1987;28:1268–1274.
24. Kiss CG, Barisani-Asenbauer T, Maca S, Richter-Mueksch S, Radner W. Reading performance of patients with uveitis-associated cystoid macular edema. *Am J Ophthalmol.* 2006;142:620–624.
25. Kiss CG, Barisani-Asenbauer T, Simader C, Maca S, Schmidt-Erfurth U. Central visual field impairment during and following cystoid macular oedema. *Br J Ophthalmol.* 2008;92:84–88.
26. Tezel TH, Del Priore LV, Flowers BE, et al. Correlation between scanning laser ophthalmoscope microperimetry and anatomic abnormalities in patients with subfoveal neovascularization. *Ophthalmology.* 1996;103:1829–1836.
27. Schneider U, Inhoffen W, Gelisken F, Kreissig I. Assessment of visual function in choroidal neovascularization with scanning laser microperimetry and simultaneous indocyanine green angiography. *Graefes Arch Clin Exp Ophthalmol.* 1996;234:612–617.